Automatic Segmentation of Abdominal Aortic Aneurysm from Magnetic Resonance Images Based on Active Shape Models and Texture Models

J. Tarjuelo-Gutierrez, B. Rodriguez-Vila, E.J. Gómez
ETSI de Telecomunicación, Universidad Politécnica de Madrid
Bioengineering and Telemedicine Centre
Biomedical Research Networking center in Bioengineering, Biomaterials and Nanomedicine (CIBER-BBN)
Madrid, Spain
jtarjuelo@gbt.tfo.upm.es

Abstract— **A semi-automatic segmentation algorithm for abdominal aortic aneurysms (AAA), and based on Active Shape Models (ASM) and texture models, is presented in this work. The texture information is provided by a set of four 3D magnetic resonance (MR) images, composed of axial slices of the abdomen, where lumen, wall and intraluminal thrombus (ILT) are visible. Due to the reduced number of images in the MRI training set, an ASM and a custom texture model based on border intensity statistics are constructed. For the same reason the shape is characterized from 35-computed tomography angiography (CTA) images set so the shape variations are better represented. For the evaluation, leave-one-out experiments have been held over the four MRI set.**

Keywords- segmentation, abdominal aortic aneurysm, intraluminal thrombus, active appearance models.

I. INTRODUCTION

An aortic aneurysm is a localized dilation of the aorta that can be found anywhere in the artery, the most common being the abdominal aortic aneurysms (AAA) [1]. It is possible that blood stagnates in the dilation, inducing intraluminal thrombus (ILT) formation [2]. Being so, three different structures can be observed in the aorta zone where the aneurysm is present: wall, ILT and lumen

Most publications on computerized AAA segmentation have concentrated on segmentation of the contrast-filled lumen. In the last years, several authors have proposed methods for segmenting the aortic wall. Subasic et al. propose a technique based on the active contour approach and another approach based on 3-D deformable model and level-set [3-4], both using CTA images. A different approach is proposed by de Bruijne et al. as they use model-based segmentation, using both CTA and MR images [5-6]. However, these works do not distinguish between the internal structures present in the AAA. This issue is treated in this work.

Automation is necessary to cope with the amount of data to process and with the low quality of images as for human experts it is highly time consuming, and will inherently introduce variability in their decisions. Furthermore, structures of interest show weak contrast and high noise at boundaries since they are made of anatomical tissues mixtures.

The objective is constructing an automatic algorithm for segmenting these three structures independently. The lumen is segmented using a contrast-filled image. The wall is segmented using ASM and a custom texture model. The ILT is the space that lies between the lumen and the wall segmentation. This segmentation is used to construct an automated patient-specific model of the aortic anatomy, to be used for guidance of catheters for treating AAA. The model distinguishes among the different anatomic structures present in the AAA.

II. MATERIALS AND METHODS

The model patient-specific is built from 3D images of the patient, composed of axial slices of the vessel, where lumen, wall and ILT are visible. The lumen is segmented in a semi-automatic way from contrast-filled images using intensity-based level sets. The main challenge is performing an automatic segmentation for the aortic wall and the ILT, which is able to distinguish between both structures.

When segmenting anatomical structures, it is common to deal with complex and variable structures. In the abdominal zone there is a wide set of different tissues that overlap and are hardly distinguishable in medical images. Model-based methods offer solutions to these difficulties by using prior knowledge of the problem. The original ASM scheme was proposed by Cootes and Taylor [7], and the main idea is generating models that represent realistically the "legal" variations that may occur among the different inter-patient and intra-patient shapes of a same anatomical structure, in our case, AAAs.

The medical images chosen are MR images. The principal reason for this choice is that MRI make possible to distinguish between the structures of interest, as shown in Fig.1. Some other advantages of MR over CTA are: the lack of ionizing radiation and nephrotoxic contrast agent, increased sensitivity to endoleaks and improved soft-tissue contrast which enables assessment of thrombus consistency [8]. Although AAA may be placed in the iliac arteries, for now we are using studies starting at the bifurcation from the aorta to the iliac arteries. A general overview of the process is shown in the flow diagram in Fig.2.

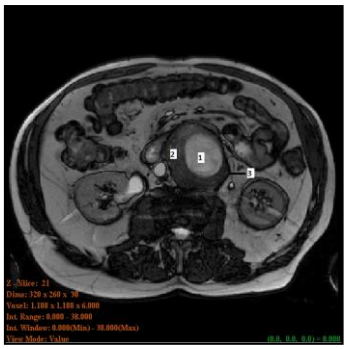

Figure. 1 Slice of a MR sequence image that has been tuned following our requirements where can be appreciated the aortic lumen (1), the thrombus (2) and the aortic wall (3).

A. *Shape and texture model training for the aortic wall*

The main challenge is performing an automatic segmentation for the aortic wall and the ILT, which is able to distinguish between both structures. To this end a model-based segmentation approach is used. In particular, we have chosen to use active shape models (ASM) and a custom texture model.

1) Active Shape Model

For constructing an ASM, it is necessary to define a training data set consisting of N manually segmented volumetric images. The simplest and most generic method to represent the shapes of the training set is a set of points distributed across the surface of the shape. These points are called landmarks and their coordinates concatenated to one vector x describe the shape.

$$x = (x_1, y_1, z_1, \dots, x_N, y_N, z_N)^T \ (1)$$

Shape variations in a training set are described using a Point Distribution Model (PDM). The shape model is used to generate new shapes, similar to those found in the training set, that are fitted to the data using a model of local grey value structure.

a) Alignment

The first step is aligning the shapes. This has to be done by translating, rotating and scaling the shapes so they are represented in the same coordinate frame. Every shape in the set is placed so that the centroid of structures inside the wall (lumen and ILT whenever it is present) is placed at the physical coordinates (0,0,0).

b) Variation modes selection

Once aligned, the next step is finding the modes of variation that better represent the variability present in the training set. Principal Component Analysis (PCA) is used to capture the statistics of the set. The basic idea behind PCA is to establish, from a training set, the pattern of "legal" variations over the shapes. One of the main restrictions of the approach, however, is the need to establish a correspondence of points. The mean shape is calculated and used to obtain the covariance matrix of the set. The main modes of variation of the set are computed from the covariance matrix of data vectors and its eigenvalues and eigenvectors are determined (eq. 2), where *S* is the covariance matrix, ϕ_k are the eigenvectors and λ_k are the eigenvalues. Each eigenvector is associated to its eigenvalue.

$$S\phi_k = \lambda_k \phi_k \ (2)$$

The eigenvectors give the modes of variation, and the eigenvalues determine the variance per mode. If ϕ contains the *t* eigenvectors corresponding to the larges eigenvalues, any of the training set *x* can be approximated by using eq. 3

$$x \approx \bar{x} + \phi b \ (3)$$

b is a vector that defines a set of parameters of a deformable model and is given by eq. 4

$$b = \phi^T (x - \bar{x}) \ (4)$$

In order to generate plausible shapes, *b* has to be costrained to be in a hyperellipsoid, (eq. 5), where the threshold M_t is chosen using the χ^2 distribution.

$$\left(\sum_{i=1}^{t} \frac{b_i^2}{\lambda_i} \right) \leq M_t \ (5)$$

a) Enlarging variations

The quantity of available training data is a key factor for the robustness of a statistical model. In our case, when working with 3D images, this quantity is almost always too low. This is due to the fact that rarely are enough images available to construct the training set, and they require a manual segmentation which is very time-consuming. This results in over-constrained models which do not represent the data in a reliable way. In order to increase model flexibility we have followed the extending PDMs strategy presented by de Bruijne et al. in [9]. Shape model flexibility is increased, for tubular objects, by modeling the axis deformation independent of the cross-sectional deformation, what improves the ability of the model to generalize to unseen shapes. Thus, we work with these models separately, as the straightened ASM models the inflation of the aneurysm and its location independently from the actual curvature of the aorta, what has empirically proved to provide better results than combining the models.

2) Texture model

As mentioned, the available training set of MRI is much reduced. For this reason applying the standard Active Appearance Model (AAM) proposed by Cootes and Taylor [10], as we have insufficient data to construct a robust texture model from training images.

Another approach to this problem is proposed, based on the work by Bailleul et al. [11].This approach consists of extracting intensity features of the border from the training data in the areas surrounding the target structure. The characteristic region is chosen as 5x5 pixels in the same slice around each landmark,. The algorithm must distinguish between internal pixels (corresponding to structures inside the arotic wall) and external pixels (corresponding to the aortic wall itself and the adjacent structures out of it). Pixels inside the characteristic region are classified depending on the distance from each point to the centroid of the internal structure. If it is lower than the distance from the landmark to the centroid, they are classified as internal, being external otherwise.

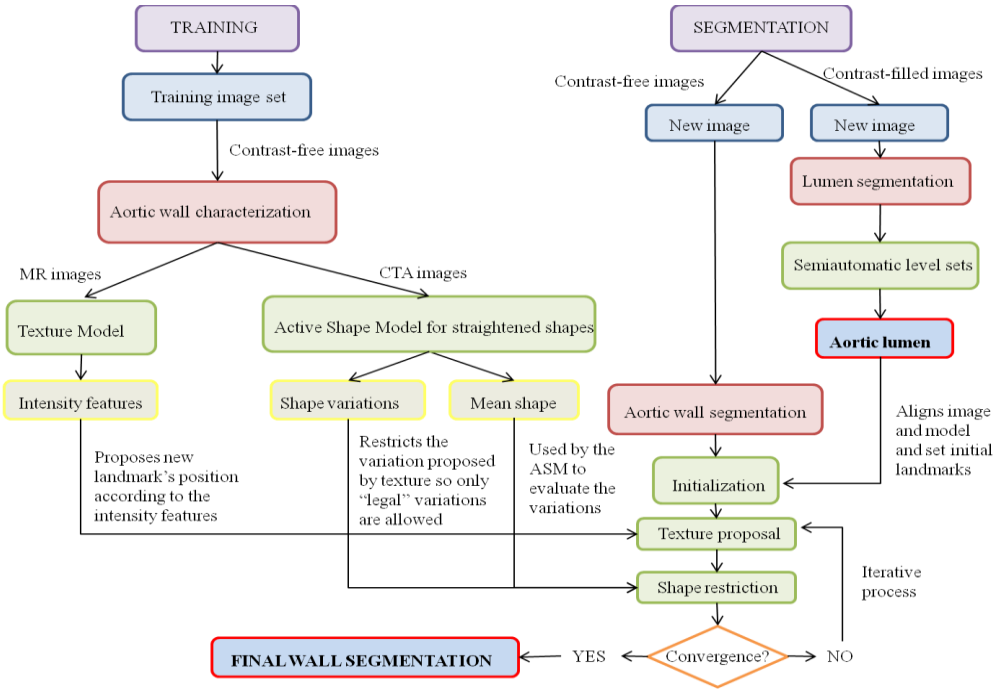

Figure. 2 Flow diagram of the model training and segmentation process.

The intensity statistics are obtained separately for internal (g_{int}) and the external (g_{ext}) pixels, as the difference among them characterizes the texture of the interest are in the image. The features have been empirically chosen by studying the training images, and they are:

- Inner/Outer means difference:

$$\overline{g_{int}} - \overline{g_{ext}} \quad (6)$$

- Inner/Outer minimums difference:

$$\min g_{int} - \min g_{ext} \quad (7)$$

- Landmark intensity/Outer minimum difference:

$$g_{landmark} - \min g_{ext} \quad (8)$$

- Outer standard deviation:

$$\sigma_{g_{ext}} \quad (9)$$

- Outer/Inner standard deviation difference:

$$\sigma_{g_{ext}} - \sigma_{g_{int}} \quad (10)$$

In order to be able to combine these different measures, they have to be normalized. This normalization is performed by using a lower quantile of 10% and an upper quantile of 90%, removing this way possible spurious peak values. The intensity features have been set such that the maximization of the normalized sum of the normalized intensity statistics indicates the best new position for the current landmark.

B. *New image segmentation process*

1) *Segmentation of the lumem*

The segmentation of the lumen is performed using MR images with contrast which are also specific for the patient. A problem that appears when using this kind of images is that the contrast masks the structures that lie close together to the lumen. The segmentation is a semiautomatic process as the intensity-based level sets method used [12] requires an initialization consisting on placing a seed (or several) over the desired structure. From this segmentation, a set of landmarks are obtained in order to initialize the segmentation of the wall.

2) *Application of the model*

Once both shape and texture have formed a model, it can be applied to segment a new image. As mentioned above, the lumen segmentation is available from a semiautomatic process. The centroid of the lumen segmentation at the bifurcation slice is obtained, and in order to perform a initial alignment of the image and the model, this point is translated to the image physical coordinate origin (0,0,0), as presented in section A.1.a. When aligned, the lumen landmarks are loaded over the new image, setting the start position for the landmarks of the wall. 5x5 pixels regions are defined centered on each landmark. Each point of this region is a candidate for being the new position of the landmark. The texture values of each candidate point are obtained as in the training step. The texture model will propose the pixel where the sum of the intensity features is higher as new position for the landmark.

Once the texture model has proposed its candidate's positions, these points are straightened and evaluated by the straightened shape mode to ensure if the variation proposed by the texture is considered as "legal" variation by the ASM. If the variation is approved, the positions of the landmark change to the new proposal. Otherwise, if the variation is excessive regarding to the ASM, it replaces the candidate points to their closest "legal" position. Then the points are returned to their pre straightened positions. This process is iterative, and converges when the texture model proposes no position changes, or when the proposals are negligible.

III. EXPERIMENTS

Leave-one-out experiments are performed on the 4 MR studies of different patients available. Leave-one-out involves using a single observation from the original sample as the validation data, and the remaining observations as the training data. This is repeated such that each observation in the sample is used once as the validation data.

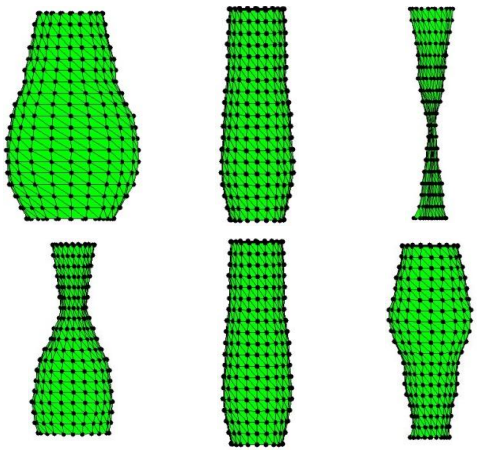

Figure. 3 Two principal modes of variation for an ASM of the AAA for straightened shapes (upper row) and combined axis and straightened (lower row). The eigenmodes' variation is computed between $\pm 2\sqrt{\lambda_m}$.

IV. RESULTS AND DISCUSION

As mentioned before, the shape training set is composed by 35 CTA images. The number of significant modes of variation of the axis and the straightened shapes model are 4 and 5, respectively. Fig. 3 shows the two principal modes of variation of the straightened shapes between $\mp 2\sqrt{\lambda_m}$.

Results of the first iteration of the segmentation algorithm are presented on Fig. 4. The initial positions are shown on the left, the texture proposals in the middle, and the ASM restricted positions are shown on the right. As appears on the figure, the initial landmarks are not located exactly in the lumen contour, since the contrasted image and the final image are not perfectly registered. The texture model proposes better positions for the landmarks, looking for the internal side of the aortic wall, and the ASM restricts the shape so avoiding illegal variations.

Although the set of images is very short, the initial results seem very promising, and the segmentation of the inner side of the aortic wall seems affordable.

V. CONCLUSIONS AND FUTURE WORKS

A semi-automatic segmentation algorithm for AAA based on ASM and texture models is proposed. The texture of the training images is characterized and a set of statistic features are obtained in order to guide the search of the structures of interest. The proposals of texture are restricted by the ASM. Leave-one out experiments have been carried over the available image set.

Future works are oriented to the complete evaluation of the whole segmentation method, and its extension to the segmentation of the outer side of the aortic wall.

ACKNOWLEDGMENT

This work is partially funded by SCATh project, FP7-ICT-2009-4-248782. The authors acknowledge Dr. Peter Verbrugghe from UZ Leuven for providing the MR images, Dr. José Luis Rodríguez Eyre from Hospital Universitario de la Princesa, Madrid for providing the CTA images and Fernando García and Alberto Lago from UPM for their invaluable assistance.

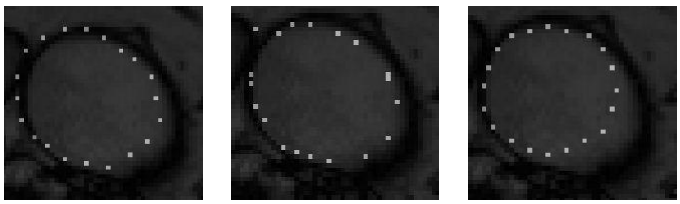

Figure. 4 Initial positions of the landmarks (left), texture landmarks proposal (center), ASM restricted landmark positions after one iteration (right).

REFERENCES

[1] A.S. Fauci, E. Braunwald, D.L. Kasper, S.L. Hauser, D.L. Longo,and J.L. Jameson, J. Loscalzo, "Harrison's Manual of Medicine," 17th ed., McGrawHil, 2009.

[2] P. Gloviczki, and J.J.I.I. Ricotta, "Aneurysmal vascular disease," In: Townsend CM, Beauchamp RD, Evers BM, Mattox KL, eds. Sabiston Textbook of Surgery. 18th ed., Philadelphia, 2007.

[3] M. Subasic, D. Kovacevic, and S. Loncaric "Segmentation of abdominal aortic aneurysm using deformable models," Technical report, Faculty of Electrical Engineering and Computing, University of Zagreb, 2000.

[4] M. Subasic, S. Loncaric, and E. Sorantin, "3D image analysis of abdominal aortic aneurysm," In: Sonka, M., Fitzpatrick, M. (eds.) Medical Imaging: Image Processing, Proceedings of SPIE, vol. 4684, pp. 1681–1689. SPIE Press, Bellingham, 2002.

[5] M. de Bruijne, B. van Ginneken, W.J. Niessen, M. Loog, and M.A. Viergever, "Model-based segmentation of abdominal aortic aneurysms in CTA images," In: Proc. SPIE Med. Imaging, vol. 5032, pp. 1560–1571. 2003.

[6] M. de Bruijne, B. van Ginneken, L. Bartles, M. van der Laan, J. D. Blankensteijn, W. J. Neissen, and M. Veirgever, "Automated segmentation of abdominal aortic aneurysms in multi-spectral MR images", Proc. MICCAI, vol. 2879, pp.538 - 545 , 2003.

[7] T.F. Cootes, C.J. Taylor, D.H. Cooper, and J. Graham, "Active shape models–their training and application," Computer Vision and Image Understanding, vol 61(1), pp.38–59, 1995.

[8] S. Haulon, C. Lions, E. McFadden, M. Koussa, V. Gaxotte, P. Halna, and J. Beregi, "Prospective evaluation of magnetic resonance imaging after endovascular treatment of infrarenal aortic aneurysms," European Journal of Vascular and Endovascular Surgery, vol 22(1),. pp. 62–69, 2001.

[9] M. de Bruijne, B. van Ginneken, M.A. Viergever, and W.J. Niessen, "Adapting active shape models for 3D segmentation of tubular structures in medical images," In: Taylor, C.J., Noble, J.A. (eds.) IPMI 2003. LNCS, vol. 2732, pp. 136–147. 2003.

[10] T.F. Cootes, and C. Taylor, "Statistical models of appearance for computer vision," Tech. rep., University of Manchester, Wolfson Image Analysis Unit, Imaging Science and Biomedical Engineering, Manchester M13 9PT, United Kingdom. 2004.

[11] J. Bailleul, S. Ruan, D. Bloyet, and B. Romaniuk, "Segmentation of anatomical structures from 3D brain MRI using anatomically-built statistical shape models," Proc. ICIP, vol 4, pp. 2741-2744. 2004.

[12] P.A. Yushkevich, J. Piven, H. Cody, S. Gee, and J.C. Gerig, "User–Guided Level Set Segmentation of Anatomical Structures with ITK-Snap," Insight J. and Proc. ISC/NAMIC/MICCAI Workshop Open-Source Software. 2005.